Regular Article

INORGANIC CHEMISTRY RESEARCH
Published by the
Iranian Chemical Society
www.inorgchemres.org
info@inorgchemres.org

Inorg. Chem. Res., *Vol. 4, No. 1, 66-75, July 2020*
DOI: 10.22036/icr.2020.233673.1069

Effect of Temperature and Reaction Time on the Morphology and Phase Evolution of Self-assembled $Cu_{7.2}S_4$ Nanospheres Obtained from Nanoparticles and Nanorods Synthesized by Solvothermal Method

Z. Rafiee and F. Davar*

Department of Chemistry, Isfahan University of Technology, Isfahan, Iran

(Received 2 June 2020, Accepted 3 July 2020)

In this research, self-assembled copper sulfide nanospheres were synthesized by the solvothermal method and the effects of reaction parameters, including reaction time and reaction temperature on the morphology and phase evolution of copper sulfide nanostructures were investigated. For the identification of copper sulfide nanostructures, X-ray diffraction (XRD), infrared spectroscopy (FT-IR), field emission scanning electron microscopy (FE-SEM), and elemental analysis (EDX) were used. The results showed that the temperature of 200 °C for 24 h is sufficient for the formation of the pure hexagonal $Cu_{7.2}S_4$ phase. The $Cu_{7.2}S_4$ nanostructures have a spherical morphology that formed from the self-assembly of the nanoparticles. Finally, the photocatalyst efficiency of $Cu_{7.2}S_4$ sphere was investigated.

Keywords: Copper(II) sulfide, Solvothermal, Morphology changes, Self-assembly

INTRODUCTION

Among of copper sulfide nanostructure, CuS, $Cu_{1.8}S$, $Cu_{7.2}S_4$, Cu_9S_5 and Cu_2S are used as a p-type semiconductor with flexible stoichiometries [1]. Copper sulfide is used as a prominent photocatalyst for the degradation of pollutants in industrial wastewater [2]. There are several methods for synthesis of copper sulfide nanostructures, including solvothermal [3], hydrothermal [4], sonochemical [5], sol-gel [6], chemical vapor deposition [7], physical vapor deposition, microemulsion [8-10], *etc.*

Copper Sulfide with different self-assembled and self-organized morphologies, including flower structures [11,12] nanowires [13], microspheres [14], nanorods [15], nanotubes [16] and flakes [17] has been obtained up to now. These types of morphologies have been used in lithium-ion batteries [18], solar cells [19], catalysts [20,21] nanometer-scale switches [22] , photothermal conversion [23], low-temperature superconductors [24], *etc.* Self-organization is a bulk union of molecules in a definite general form/shape but with an unsystematic distribution at the molecular level; on the other hand, self-assembly is a particular combination of molecules in a limited form/shape driven by particular intermolecular interactions.

The photocatalytic degradation of dyes using photoactive materials in aqueous solutions mainly depends on the morphology and size of nanocatalysts, intensity of light, concentration of dyes, band gap of semiconductor, amount of photocatalyst, and surface area of catalyst [2,25-29]. Photocatalytic activity of copper sulfide was investigated by different groups [28-39]. Li *et al.* roported the preparation of hierarchical structures of copper(II) sulfide nanomaterials by solvothermal method and their application in the photocatalytic degradation of methylene blue [30]. Ghosh and Mondal prepared Cu_7S_4 thin film by electrochemical method. The band gap of the as-obtained thin film was calculated to be 1.95 eV. Such films can be used as photocatalysts to remove rhodamine B (RB) dye pollutants [31]. Shen *et al.* studied the synthesis and characterization of self-assembly of CuS nanoflakes into flower-like microspheres [3]. However, up to now, there is

*Corresponding author. E-mail: davar@iut.ac.ir

no report on the synthesis of self-assembled $Cu_{7.2}S_4$ nanospheres by solvothermal method using copper(II) acetylacetonate instaed of copper(II) acetate as the copper source and elemental sulfur as the sulfur source. Finally, the photocatalytic activity of the self-assembled $Cu_{7.2}S_4$ nanospheres was studied on the degradation of methylene blue as a model.

EXPERIMENTAL

Materials

copper(II) acetate monohydrate $Cu(OAc)_2.H_2O$, acetylacetone (acacH), elemental sulfur, absolute ethanol, and oleic acid were purchased from Merck Company. Copper(II) acetylacetonate [$Cu(acac)_2$] was prepared according to Ref. [39].

Synthesis of the Self-assembled Copper Sulfide Nanostructures

2 mmol of the precursor $Cu(acac)_2$ was mixed with 10 ml of oleic acid. Then, 2 mmol of sulfur powder was added to the solution in 300 ml Teflon lined autoclave and kept at different reaction times (6-24 h) and temperatures (105-200 °C). The black precipitation was centrifuged several times, washed with ethanol, and dried in an oven at 60 °C for 24 h. The effects of the reaction parameters, including reaction temperature and reaction time, are summarized in Table 1.

Photocatalytic Degradation of MB

The photocatalytic reaction was performed using 15, 25 and 45 mg copper sulfide nanostructures in separate quartz beakers mixed with 50 ml of methylene blue (MB) solution containing 6 ppm MB for 10 min. The solution was then placed at a distance of 50 cm from a UV lamp. Each 10 min, 3 ml of the solution was separated, and the absorption was measured by UV-Vis at wavelengths 200-800 nm. The degradation percent of the dye was determined by equation (2). C_0 and A_0 are the initial concentration of the dye and the absorption of the dye solution before the irradiation, respectively. C_t and A_t are the concentration and the absorption of the dye solution after the radiation, respectively.

Characterization Equipments

FE-SEM images were recorded by a TESCAN model device from CZECH company. FT-IR spectra of copper sulfide nanostructures with KBr pellets were recorded by a 680-PLUS spectrophotometer in the region of 400-4000 cm^{-1}. X-ray diffraction (XRD) pattern was performed on an X-Pert Pro-MPD Philips using Cu k_α radiation $\lambda = 0.15406$ nm as the X-ray source.

RESULTS AND DISCUSSION

X-ray Diffraction Pattern

Investigating of the reaction temperature and time. Figure 1 shows the X-ray diffraction (XRD) pattern of sample S_1 prepared at 105 °C for 6 h. According to this figure, the sample is not pure and has four different phases (Cu_2S, Cu_7S_4, Cu_8S_5 and elemental sulfur). The Miller's indices related to the crystalline planes for each of the peaks are shown in Fig. 1a.

The XRD pattern of sample S_5 prepared at 200 °C for 12 h is shown in Fig.1b, which indicates the reflections at 27.6, 31.9, 45.91 and 54.2° attributed to $Cu_{7.2}S_4$ phase (JCPDS card No. 00-024-0061) with a cubic crystal structure and lattice parameters of $a = b = c$ =5.75 Å. Moreover, the reflections at 39.2, 48.4 and 67° correspond to the tetragonal $Cu_{1.81}S$ phase with the lattice parameters of $a = b$ = 1.8340 Å and c = 7.5580 Å.

The XRD pattern of sample S_6 is shown in Fig. 1c. According to this figure, the reflections at 27.6, 31.9, 45.91 and 54.2° are matched to digenite phase and cubic crystal structure of $Cu_{7.2}S_4$ (JCPDS card NO of 01-072-1966) with network parameters $a = b = c$ = 5.5770 Å .

FE-SEM Images

Effect of temperature on the morphology of the samples. Figure 2a shows the FE-SEM images of sample S_2 prepared at 105 °C. In this image, an irregular shape with different morphologies is observed. It may be due to the presence of various phases of copper sulfide existed in this sample, which was previously confirmed by the XRD analysis. Figure 2b shows the FE-SEM images of sample S5 prepared at 200 °C for 12 h. According to this figure, the spheres smaller than one micrometer, self-assembled from tiny nanoparticles, are observed.

Table 1. Samples Code Table for Synthesized by Solvothermal (S) Method

Sample code	Cu^{2+}: S mol ratio	Oleice acid (ml)	Temperature (°C)	Time (h)
S_1	1:1	10	105	6
S_2	1:1	10	105	12
S_3	1:1	10	200	6
S_4	1:1	10	200	10
S_5	1:1	10	200	12
S_6	1:1	10	200	24

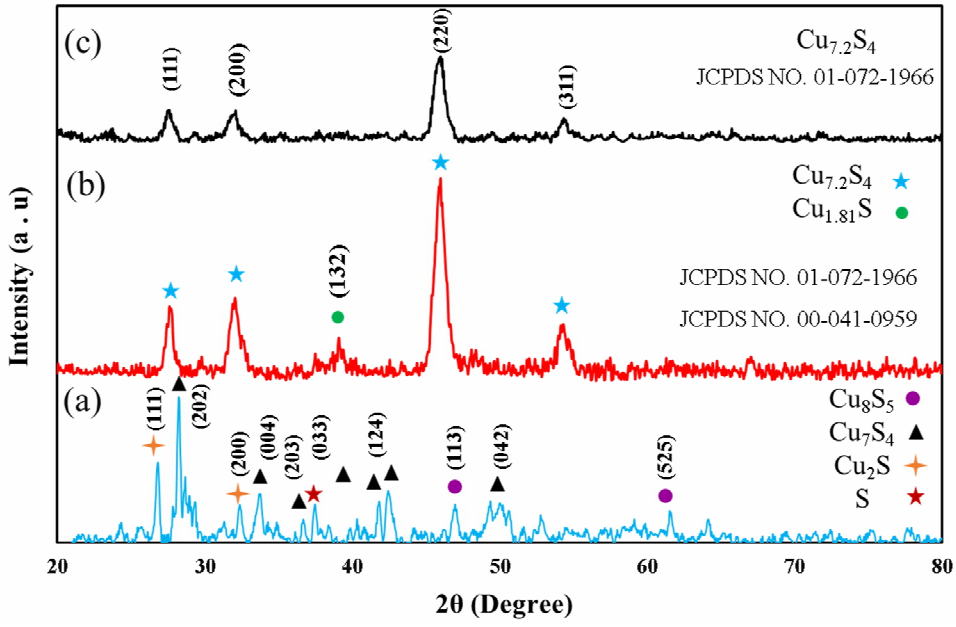

Fig. 1. XRD pattern of different samples (a) S_1, 6 h at 105 °C,; (b) S_5, 12 h at 200 °C; and (c) S_6, 24 h at 200 °C.

Effect of reaction time on the morphology of the samples. Figure 3a shows the FESEM image of sample S_3 prepared at 200 °C for 6 h. There are microspheres self-assembled from the fine particles, which are similar to Fig. 2b (S_5 sample).

When the reaction was performed at 200 °C for 10-24 h in samples S_4 and S_6, a mixture of spheres self-assembled from the nanorods and nanoparticles was observed. The nanorods have a diameter of 20 nm. In fact, for the formation of hierarchical structures of copper(II) sulfide,

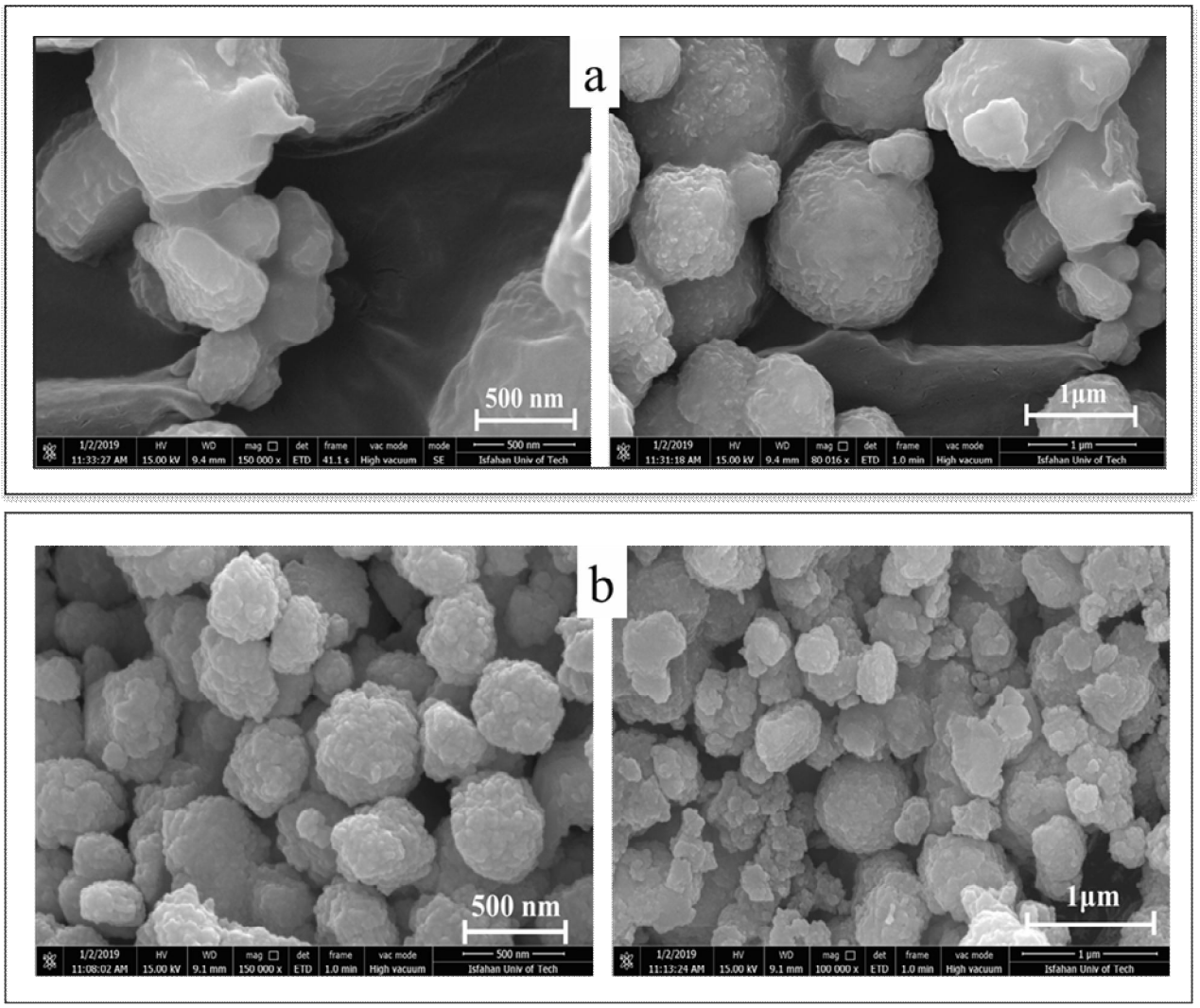

Fig. 2. SEM images of copper sulfide nanostructures synthesized at different temperatures (a) S_2,12 h at 105 °C; and (b) S_5,12 h at 200 °C.

two steps probably are taken. The first stage is the heterogeneous growth and creation of the nanorod structural units, and the second stage is the macroscopic assembly of copper(II) sulfide hierarchical structural units to the microspheres (Figs. 3b and 3c) [30]. Figure 3c shows that with increasing the reaction time, the particles and rods on the spheres have been grown. S_6 sample prepared at 200 °C for 24 h consists of the microspheres self-assembled from the nanoparticles and nanorods with size ranges of 25-30 nm. This observation is in good agreement with the Ostwald ripening [40].

FT-IR Spectra

According to the FTIR spectrum of the precursor $Cu(acac)_2$ (Fig. 4a), the bands at 454 and 612 cm^{-1} are related to the vibration of Cu-O bonds, as well as the bands at 1020, 1190 and 1274 cm^{-1} are related to the C-O stretching vibration. The band at 1412 cm^{-1} is assigned to the vibration of C=C. The bands at 1577 and 1530 cm^{-1} are related to the asymmetric and symmetric vibration of the

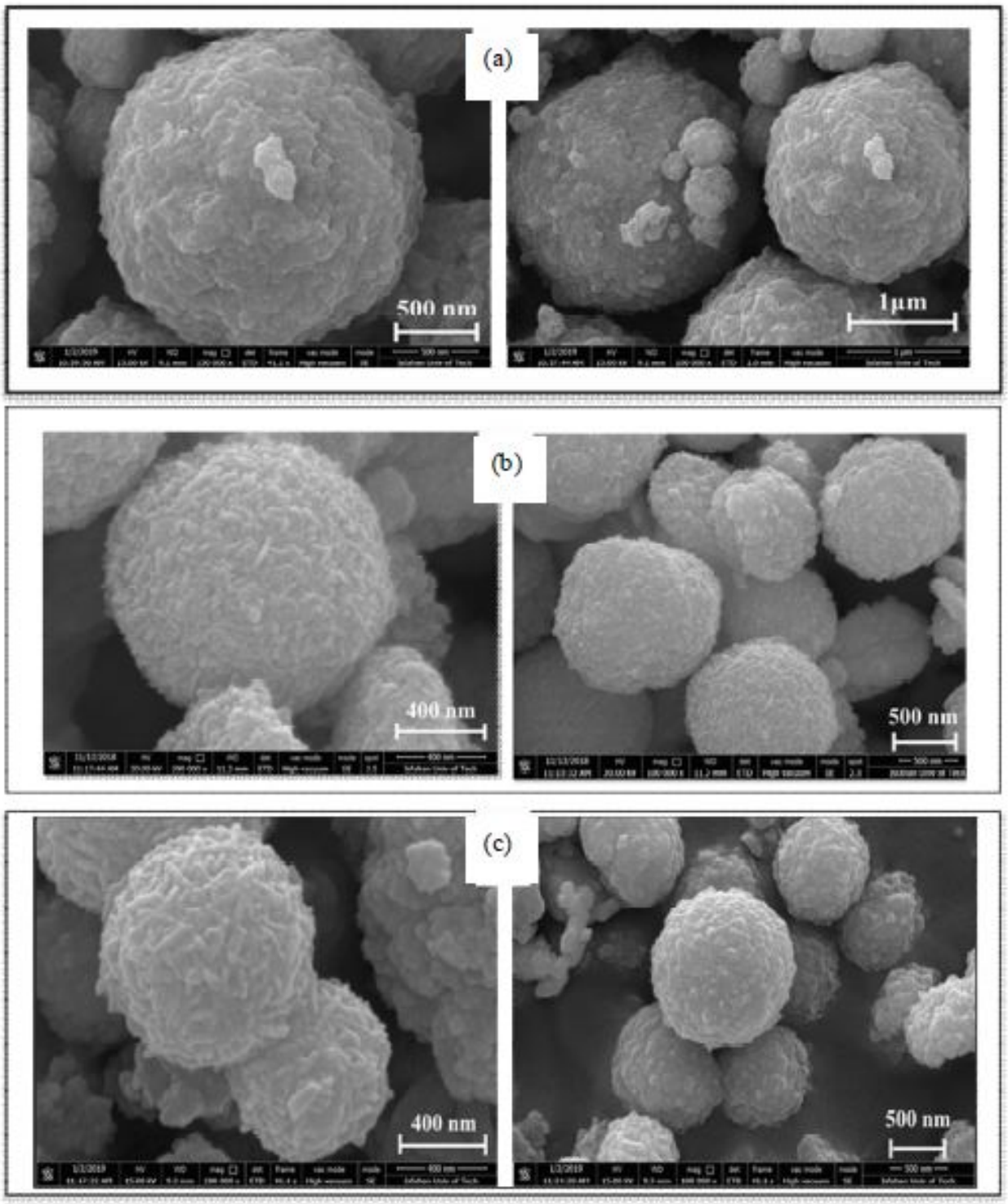

Fig. 3. FE-SEM images of samples synthesized at different times, (a) S_3, 6 h at 200 ℃, (b) S_4,10 h at 200 ℃,(c) S_6, 24 h at 200 ℃ .

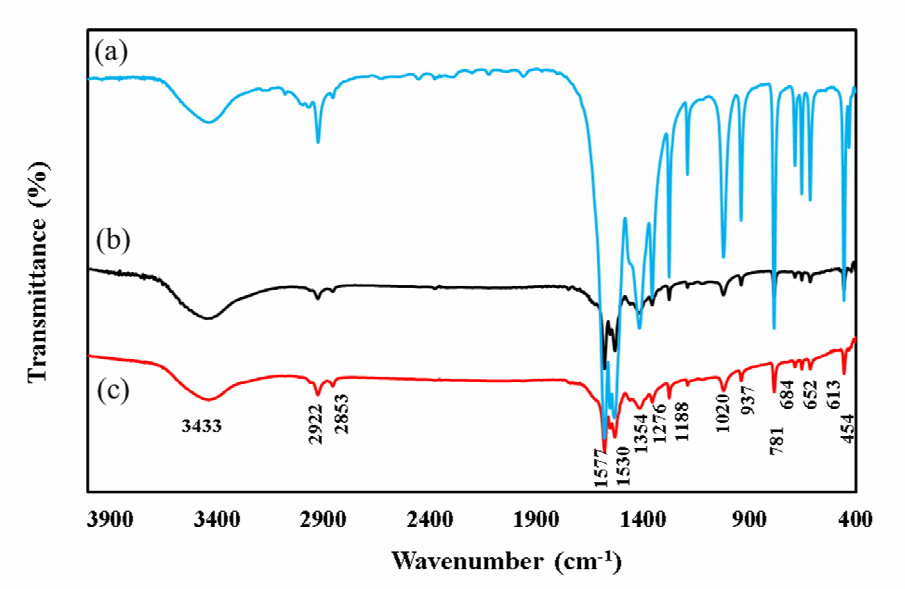

Fig. 4. FT-IR Spectra of (a) $Cu(acac)_2$ precursor; (b) S_1, 6 h at 105 °C; and (c) S_2, 12 h at 105 °C.

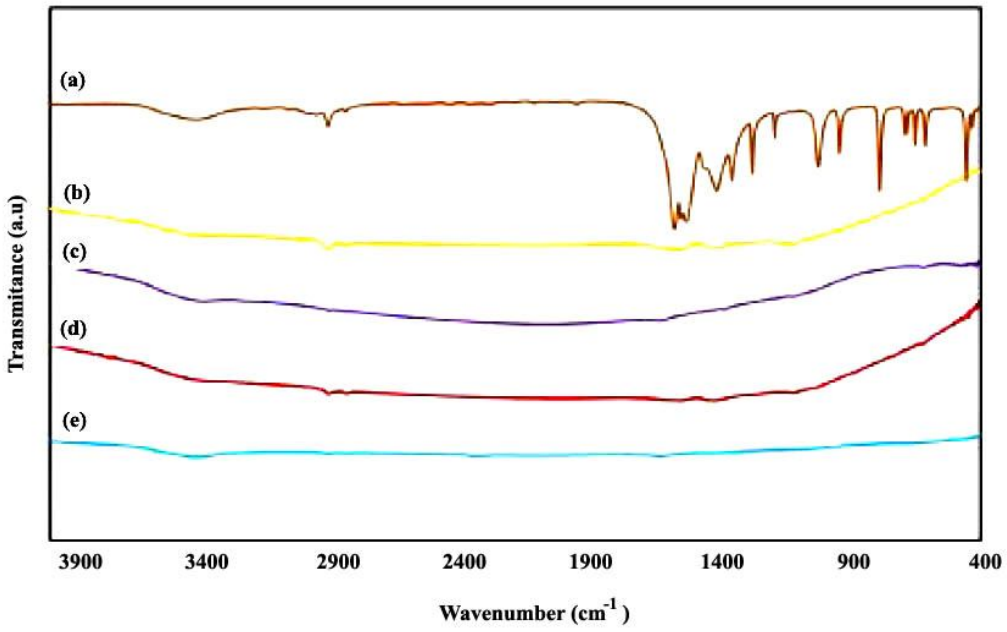

Fig. 5. FT-IR Spectra of (a) $Cu(acac)_2$ precursor, (b) S_3 ,6 h at 200 °C; (c) S_4 , 10 h at 200 °C; (d) S_5 , 12 h at 200 °C; and (e) S_6, 24 h at 200°C.

-COOH group. The vibration bands at 2922 and 3433 cm^{-1} are related to the stretching vibration of C-H and the adsorbed water molecules, respectively [40-42].

According to Figs. 4b and 4c, the sample prepared at 105 °C has absorption bands in the regions of 1530-1577 and 1020-1354 cm^{-1}, that confirm the presence of $Cu(acac)_2$

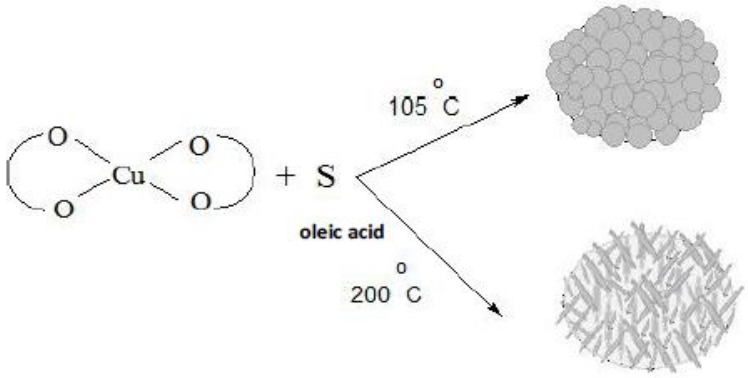

Fig. 6. Schematic of the formation mechanism of self-assembled copper sulfide spheres.

and incompletete formation of pure copper(II) sulfide. Figures 5b-f shows the FT-IR spectra of the samples prepared at 200 °C in different reaction times. By comparison of Fig. 5a (FTIR of the copper complex) and Fig. 5b-f, it can be observed that a large extent of the copper complex as impurities, related to the presence of $Cu(acac)_2$ in the product, was removed. Thus, the optimum reaction temperature for the preparation of copper(II) sulfide is 200 °C.

By observing Figs. 5d and 5e, the absence of sharp bands in the range of 1000-1500 cm^{-1} is due to the absence of acetylacetone in the precursor ($Cu(acac)_2$). The presence of bands at 2920 and 2851 cm^{-1} in Figs. 5b-e indicates the presence of oleic acid in the sample [43].

The self-assembly can be done statically or dynamically. In static self-assembly, the thermodynamic equilibrium creates a system-forming approach so that the free energy of the particle surface is reduced. However, in dynamic self-assembly, system components are put together by a specific local interaction and are named “self-organized”. In this work, the self-assembly of tiny spherical or rod-like morphology was caused to obtain the copper sulfide microspheres. When the "acac" ligand was used, the free Cu^{2+} ions in the solution were limited to reacting with sulfur, and a diffusion-controlled mechanism was overcome at 105 °C. Generally, the nuclei in a diffusion-controlled mechanism tend to grow in a spherical morphology (Fig. 6). However, by increasing the reaction temperature to 200 °C, more "acac" degradation is occurred rapidly on the samples, and a higher amount of Cu^{2+} is present in the solution as compared to a reaction temperature of 105 °C. Thus, a surface-controlled mechanism takes place in this situation.

In the surface-controlled mechanism (anisotropic growth), due to some oleic acid molecules linked to the specific crystal plane of the initial nuclei (See Figs. 4 and 5), the resulted particle grows in one direction, and tiny nanorods are obtained. Then, due to the self-assembly of these nanorods, the microspheres self-assembled from the nanorods are formed (S_3 sample, 6 h at 200 °C). However, by increasing the reaction time from 6 to 24 h, the microspheres are self-assembled from a mixture of nanoparticles and nanorods. It is maybe due to this fact that by increasing the reaction time, some oleic acid molecules are removed from the initial copper sulfide nuclei, and no preferred particle growth has occurred for some CuS particles [44].

EDS Analysis

To indicated elemental analysis of copper(II) sulfide nanoparticles, energy dispersive X-ray spectroscopy was used (Fig. 7). According to EDS analysis, the presence of elements, including Cu and S is confirmed, and no other impurities are observed in this sample.

Photocatalytic activity. Sample S_3 that has a pure $Cu_{7.2}S_4$ phase with a smaller particle size was selected for the photocatalytic experiments. Figure 8 shows the UV-Vis spectra of the MB solution under the UV irradiation. The absorption spectra show a decrease in the peak intensity at 662 nm during the time. As a result, the MB concentration in the solution is decreased and indicated the degradation of

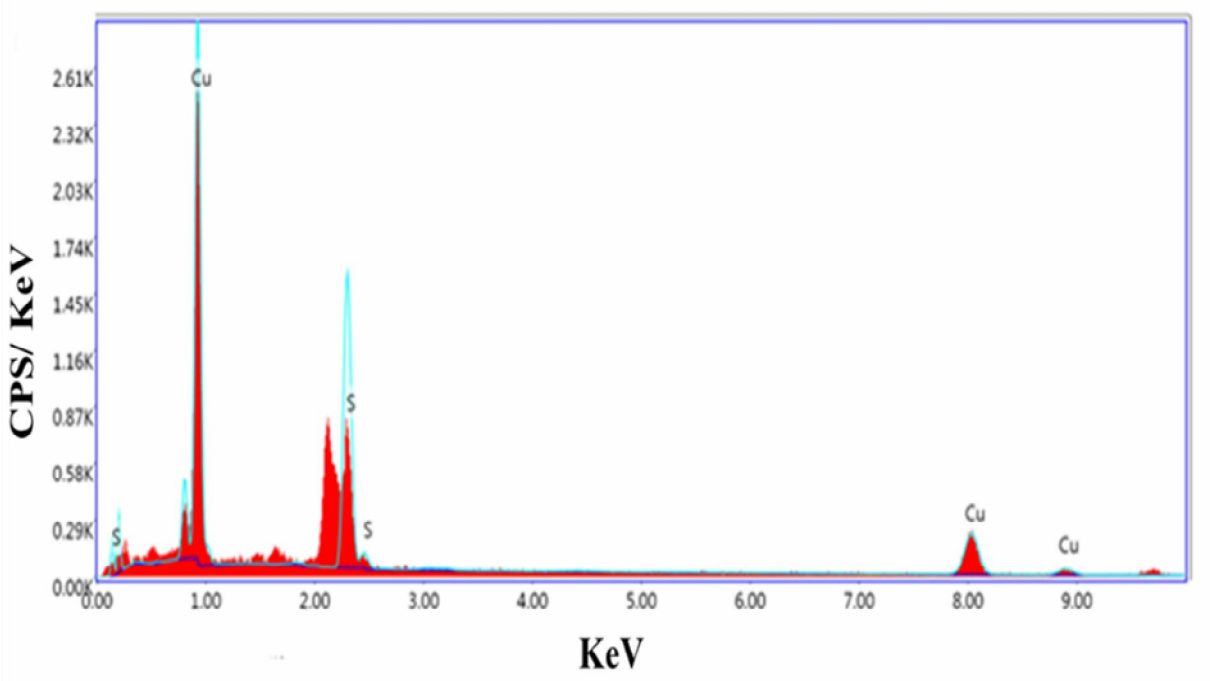

Fig. 7. EDS analysis of copper sulfide nanostructures (S_6 sample).

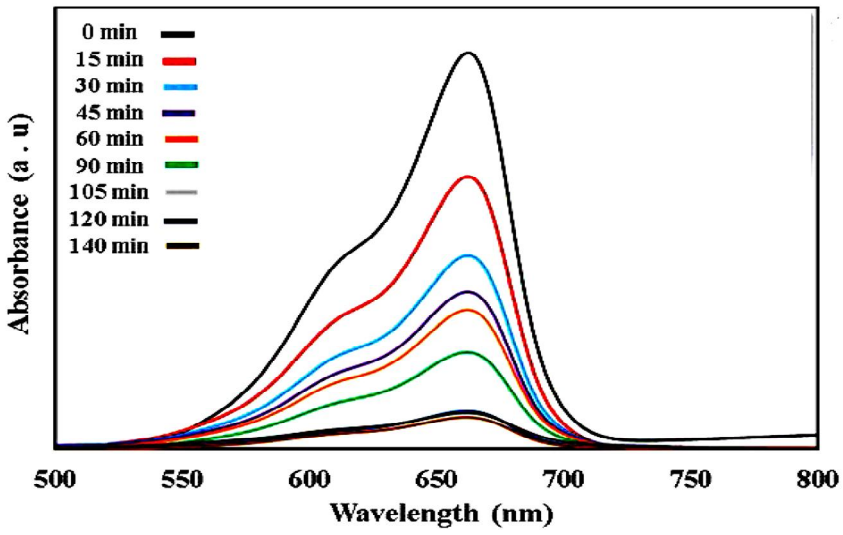

Fig. 8. UV-Visible spectra of methylene blue at different reaction times.

the dye molecules. According to the results in Fig. 9, the sample containing 45 mg of the photocatalyst has the highest percentage of MB degradation (100% degradation at 80 min). This work reveals a higher photocatalytic efficiency for the degradation of methylene blue as compared to other research [30].

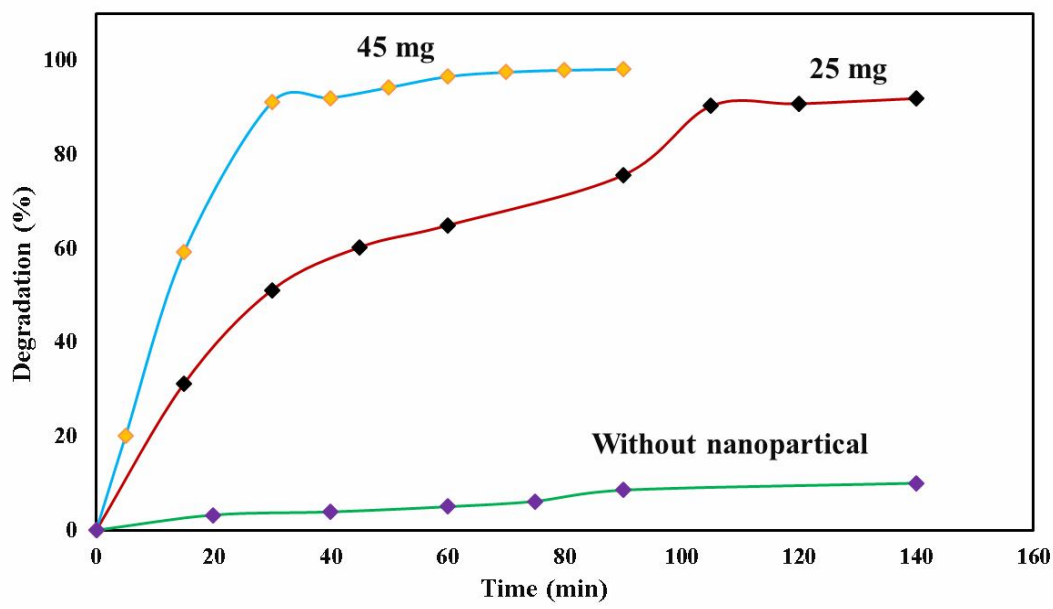

Fig. 9. Degradation of methylene blue under the UV irradiation in the presence of different amounts of the photocatalyst.

CONCLUSIONS

Self-assembled $Cu_{7.2}S_4$ nanospheres were synthesized with copper(II) acetylacetonate and elemental sulfur at 200 °C for 24 h by the solvothermal method. Results show that the degradation of "acac" ligand caused more copper ions exist in the solution, and surface-controlled growth mechanism caused anisotropic growth of sample (rod-like shape). Finally, the photocatalyst efficiency of the $Cu_{7.2}S_4$ sphere shows 100% degradation of methylene blue at 80 min.

ACKNOWLEDGMENTS

The authors of the article thank the financial support of the Isfahan University of Technology.

REFERENCES

[1] K. Mageshwari, S. Sawanta Mali, T. Hemalatha, R. Sathyamoorthy, S. Pramod Patil, Prog. Sol. State Chem. 39 (2011) 108.

[2] A. Dasari, G. Veerabhadram, Mat. Today Energy 9 (2018) 83.

[3] S. Xiao-Ping, H. Zhao, H.Q. Shu, H. Zhou, A.-H. Yuan, J. Physics Chem. Solids 70 (2009) 422.

[4] Z.C. Zhiguo, S. Wang, D. Si, B. Geng, J. Alloys Compds 492 (2010) L44.

[5] X. Jin-Zhong, S. Xu, J. Geng, G.-X. Li, J.-J. Zhu, Ultrason. Sonochem. 13 (2006) 451.

[6] R. Sana, A. Parveen, A. Azam, Perspec. Sci. 8 (2016) 632.

[7] R. Liesbeth, B. Meester, F. de Lange, J. Schoonman, A. Goossens, Chem. Mat. 17 (2005) 2724.

[8] C. Lifei, Y. Shang, H. Liu, Y. Hu, Mat. Design 31 (2010) 1661.

[9] F. Davar, M.R. Loghman-Estarki, M. Salavati-Niasari, M. Mazaheri, J. Cluster Sci. 27 (2016) 593.

[10] A. Peter, N.L. Botha, Res. Physics 6 (2016) 581.

[11] W. Huijie, Y. Li, Q. Li, Appl. Phys. A 123 (2017) 196.

[12] Y. Liu, Y. Z. Zhou, S. Zhang, W. Luo, G. Zhang, Appl. Surf. Sci. 442 (2018) 711.

[13] C.Y. Cheng, J.B. Shi, C. Wu, C.J. Chen, Y.T. Lin, P.F. Wu, Mat. Lett. 62 (2008) 1421.

[14] Z. Biao, X. Guo, Y. Zhou, T. Su, C. Ma, R.

Zhang, Cryst. Eng. Comm. 19 (2017) 2178.
[15] D. Patil, S.-H. Han, M.C. Rath, V.J. Fulari, Mat. Lett. 90 (2013) 138.
[16] T. Changhui, Y. Zhu, R. Lu, P. Xue, C. Bao, X. Liu, Z. Fei, Y. Zhao, Mat. Chem. Phys. 91 (2005) 44.
[17] S. Umair, R.A. Hussain, A. Badshah, J. Solid State Chem. 238 (2016) 25.
[18] H. Yan, Y. Wang, W. Gao, Y. Wang, L. Jiao, H. Yuan, S. Liu, Powder Technol. 212 (2011) 64.
[19] K. Rahul, A. Singh, A. Anshul, D. Mishra, S.S. Amritphale, J. Mat. Sci. Mat. Electronics 28 (2017) 5597.
[20] C. Claudia, M. Ibanez, O. Dobrozhan, A. Singh, A. Cabot, K.M. Ryan, Chem. Rev. 117 (2017) 5865.
[21] X. Wence, S. Zhu, Y. Liang, Z. Li, Z. Cui, X. Yang, A. Inoue, Scien. Reports 5 (2015) 18125.
[22] G. Wen, Y. Sun, M. Cai, Y. Zhao, W. Cao, Z. Liu, G. Cui, B. Tang, Nature Comm. 9 (2018) 1.
[23] L. Chunbo, X. Zhang, F. Xu, Y. Yuan, H. Pei, Z. Sun, L. Li, Z. Bao, Small 14 (2018) 1703077.
[24] G. Mao, W. Dong, D.G. Kurth, H. Mohwald, Nano Lett. 4 (2004) 249.
[25] L. Xin, J. Yu, M. Jaroniec, Chem. Soc. Rev. 45 (2016) 2603.
[26] T. Natarajan, T. Sivakumar, K. Natarajan, H.C. Bajaj, R.J. Tayade, J. Nanoparticle Res. 15 (2013) 1669.
[27] R. Qadeer, Q. Riaz, Colloids and Surfaces A: Physicochem. Eng. Aspects 293 (2007) 217.
[28] G. Mishra, M. Tripathy, Colourage 40 (1993) 35.
[29] D. Ayhan. J. hazard, Mat. 167 (2009) 1.
[30] L. Fei, J. Wu, Q. Qin, Z. Li, X. Huang, Powder Technol. 198 (2010) 267.
[31] G. Amrita, A. Mondal, Appl. Sur. Sc. 328 (2015) 63.
[32] Z.Y. Qiao, B.P. Zhang, Z.H. Ge, L.F. Zhu, Y. Li, Europ. J. Inorg. Chem. 2014 (2014) 2368.
[33] A. Dasari, M. Venkatesham, A.S. Kumari, G.B. Reddy, D. Ramakrishna, G. Veerabhadram, J. Exp. Nanosci. 11 (2016) 418.
[34] X. Ya-Jun, Y. Shen, X.S. Hu, S.N. Chen, J. Nanosci. Nanotechnol. 18 (2018) 1696.
[35] Z. Lijuan, L.Zhou, C. Sun, Y. Gu, W. Wen, X. Fang, Cryst. Eng. Comm. 20 (2018) 6529.
[36] H. Xiao-Sai, Y. Shen, L.H. Xu, L. Wang, L. Lu, Y. Zhang, Appl. Surf. Sci. 385 (2016) 162.
[37] L. Fei, T. Kong, W. Bi, D. Li, Z. Li, X. Huang, Appl. Surf. Sci. 255 (2009) 6285.
[38] X. Hu, X. Sai, Y. Shen, Y. Zhang, J. Nie, J. Physics Chem. Solids 103 (2017) 201.
[39] Z.Y. Cai, J.Y. Tang, G.L. Wang, M. Zhang, X. Hu, J. Crys. Growth 294 (2006) 278.
[40] A. Khorshidi, A.F. Shojaei, M. Mojallali Foumani, Iranian Polymer J. 26 (2017) 481.
[41] S. Jian, G. Yu, L. Liu, Z. Li, Q. Kan, Q. Huo, J. Guan, Catalysis Sci. Technol. 4 (2014) 1246.
[42] Y. Moreno, R. Arrue, R. Saavedra, J.Y. Pivan, O. Pena, T. Roisnell, J. Chilean Chem. Soc. 58 (2013) 2122.
[43] W.A.P.J. Premaratne, W.M.G.I. Priyadarshana, S.H.P. Gunawardena, A.A.P. De Alwis, J. Sci. Univ. Kelaniya Sri Lanka 8 (2014) 11.
[44] G. Cao, Y. Wang, Nanostructures and nanomaterials: synthesis. Properties and Applications, Imperial College Press, 2004.